

An analytical method for disentangling the roles of adhesion and crowding for random walk models on a crowded lattice

Adam J Ellery¹, Ruth E Baker², Matthew J Simpson¹

¹ *School of Mathematical Sciences, Queensland*

University of Technology, Brisbane, Australia and

² *Mathematical Institute, University of Oxford,*

Radcliffe Observatory Quarter, Woodstock Road, Oxford, UK.

The motion of cells and molecules through *in vivo* biological environments is affected by the presence of other cells and scaffolds that can act as obstacles [1–4]. Interactions between cells and obstacles can include both crowding effects [5, 6], as well as adhesion/repulsion effects [7, 8]. A great deal of theoretical progress has been made in terms of developing mathematical insight into how adhesion between motile cells impacts *in vitro* experiments without any obstacles present [9–12]. However, mathematical models describing the impact of both crowding and adhesion/repulsion *in vivo* with obstacles present are predominantly based on simulation studies, without any underlying analysis [1, 5, 13, 14].

While we anticipate that both crowding and adhesion act to impede the motion of cells *in vivo*, it is not possible to quantify the relative roles of these two mechanisms based on intuition alone. Although it is possible to perform simulations that include both crowding and adhesion, simulation studies can be time consuming, and can fail to provide more general insight. To address these limitations we consider a stochastic, lattice-based model describing the motion of an agent (e.g. a cell or biological molecule) through an environment that is randomly populated by immobile obstacles at density $\phi \in [0, 1]$. The motion of the agent is affected by crowding and adhesion/repulsion between the agent and the obstacles. The strength of adhesion/repulsion is measured by $\zeta \in [-1, 1]$: setting $\zeta = 0$ corresponds to pure crowding with no adhesion/repulsion; $\zeta > 0$ corresponds to combined adhesion and crowding; and $\zeta < 0$ corresponds to combined repulsion and crowding. We present an exact method that can be used to quantify the relative roles of crowding and adhesion/repulsion by producing exact calculations of the long time Fickian diffusivity, D , of the motile agent. Using this method we calculate $D(\phi, \zeta)$ so that we are able to quantify the roles of both crowding and adhesion/repulsion in terms of the long time Fickian diffusivity. Our results suggest that there is a threshold density of obstacles ($\phi \approx 0.3$) below which adhesion/repulsion has a negligible impact on the long time Fickian diffusivity. In contrast, above this threshold ($\phi > 0.3$), adhesion/repulsion interactions have a significant influence on the long time Fickian diffusivity. The accuracy of our exact calculations is tested using random walk simulations, and although we present results for a two-dimensional square lattice, our approach applies to any regular lattice in two or three dimensions.

We consider a square lattice with unit lattice spacing, $\Delta = 1$, and dimension $X \times Y$. Sites are indexed (i, j) so that each site has location $(x, y) = (i\Delta, j\Delta)$ with $0 \leq x \leq X - 1$ and $0 \leq y \leq Y - 1$. To initiate a simulation, lattice sites are randomly populated with immobile

and impenetrable obstacles to a spatially uniform density, ϕ , with, at most, one obstacle per site. A motile agent is placed on a vacant site, and allowed to undergo a nearest neighbor random walk in which all potential motility events that would place the agent on a site that is occupied by an obstacle are aborted [15].

During each discrete time step, of duration $\tau = 1$, the probability that the motile agent attempts to step to a randomly chosen nearest neighbor lattice site is

$$\frac{p_m}{4} \left(1 - \frac{\zeta}{3} N \right), \quad (1)$$

where $p_m \in [0, 1]$ is the probability that an isolated agent will attempt to move during a time interval of duration τ , $N = 0, 1, 2, 3$ or 4 , is the number of nearest neighbor sites occupied by obstacles, and $\zeta \in [-1, 1]$ is the adhesion/repulsion parameter. To ensure that both the net probability of movement and the net probability of remaining stationary during any time step are always greater than zero and less than unity, we consider the transition probabilities in which $N = 0, 1, 2, 3$ or 4 , separately. Solving the resulting inequality expressions leads us to include the factor of $1/3$ in Equation (1), so that $\zeta \in [-1, 1]$.

The schematic in Figure 1(a) illustrates how crowding and adhesion/repulsion are incorporated into the model. The lattice site containing the red agent is not adjacent to any obstacles ($N = 0$) and the probability that the red agent will move during a time step of duration τ is simply p_m , which is independent of ζ . Since there are no obstacles surrounding the red agent, it is able to move to any of the four nearest neighbor sites, with the target site being chosen at random. In contrast, the blue agent is adjacent to one obstacle ($N = 1$) and the probability that the blue agent will move during a time step of duration τ is $p_m (1 - \zeta/3)$, which depends on the strength of adhesion/repulsion. Therefore, the motility of agents that are adjacent to one or more obstacles are affected by the strength of adhesion/repulsion to those obstacles. If the blue agent attempts to move, the direction of movement will be chosen at random. If, in this case, the blue agent attempts to move in the positive x direction, the potential movement event will be aborted due to crowding effects caused by the obstacle.

To quantify how crowding and adhesion/repulsion affect the motility of a single motile agent, we consider performing a stochastic simulation in which we record the agent's squared displacement, $r^2(t) = x^2(t) + y^2(t)$, where $x^2(t)$ and $y^2(t)$ represent the components of the squared displacement in the x and y directions, respectively. Following earlier studies

[1, 5, 13, 14] we assume that the mean squared displacement follows a power law

$$\langle r^2(t) \rangle = (2d)\bar{D}t^\alpha, \quad (2)$$

where $d = 2, 3$ is the physical dimension, $\langle \cdot \rangle$ denotes the average over a large ensemble of identically prepared realizations, and \bar{D} is a generalized diffusivity with units $[L^2/T^\alpha]$ which is less than the diffusivity when no obstacles are present, $D_0 = p_m \Delta^2 / (2d\tau)$. The exponent α is a positive constant that can be used to classify the type of transport process taking place, with $\alpha = 1$ corresponding to Fickian diffusion and $\alpha < 1$ corresponding to subdiffusion [1, 5, 13, 14]. Rearranging Equation (2) gives

$$\log_{10} (\langle r^2(t) \rangle / t) = \log_{10} ((2d)\bar{D}) + (\alpha - 1) \log_{10} (t). \quad (3)$$

This means that if the power law in Equation (2) accurately describes the evolution of the mean squared displacement data, a plot of $\log_{10} (\langle r^2(t) \rangle / t)$ as a function of $\log_{10} (t)$ will be a straight line for all $t > 0$. If the transport process is Fickian diffusion ($\alpha = 1$) the straight line will be horizontal, with zero slope. In contrast, if the transport process is subdiffusion ($\alpha < 1$) the straight line will have negative slope.

To demonstrate these ideas we perform an ensemble of simulations without adhesion/repulsion and with $\phi = 0.2$ on a lattice with periodic boundary conditions, and we plot $\log_{10} (\langle r^2(t) \rangle / t)$ as a function of $\log_{10} (t)$ in Figure 1(b). Consistent with many previous simulation studies [1, 5, 13, 14, 16–18], we observe that $\log_{10} (\langle r^2(t) \rangle / t)$ follows a curve. Initially the curve has a negative slope, and the curve tends to a horizontal asymptote as $t \rightarrow \infty$. This suggests that the transport process becomes Fickian in the long time limit, $t \rightarrow \infty$, with a reduced Fickian diffusivity, \bar{D} . For the data in Figure 1(b), we fit a horizontal line to the data in the interval $10^3 \leq t \leq 10^4$, giving $\bar{D} \approx 0.095$. This means that the obstacles have reduced the long time Fickian diffusivity compared to the case where there are no obstacles present, $D_0 = p_m \Delta^2 / (2d\tau) = 0.25$, in this case.

Unfortunately, using stochastic simulations to compute the long time Fickian diffusivity like we did in Figure 1(b) is problematic for two reasons. First, a very large number of identically prepared realizations of the stochastic process are required to produce sufficiently smooth mean squared displacement data. Second, the Fickian diffusion regime is only reached in the long time limit, $t \rightarrow \infty$, meaning that we must perform a very large number of identically prepared realizations over a very long period of time to obtain a reasonable approximation of \bar{D} . These two issues motivate us to develop an exact calculation

of \bar{D} that does not rely on stochastic data. To calculate the long time Fickian diffusivity we modify a method originally proposed by Mercier and Slater [19–21]. Our modification to their method is to incorporate the effects of adhesion/repulsion. We will describe how to apply the method to calculate the long time Fickian diffusivity in each component direction. All of the details are given for the x Cartesian direction, and adapting the method to apply to the y and z Cartesian directions is straightforward.

To begin with we apply the Nernst-Einstein relationship, which is a special case of the fluctuation-dissipation theorem [22],

$$\bar{D}_x = D_0 \frac{\mu(\epsilon)}{\mu_0}, \quad (4)$$

where $\mu(\epsilon)$ represents the probability of movement in the positive x direction when the motion includes a bias of strength $\epsilon \ll 1$, and μ_0 is the probability of movement in the positive x direction where there is no bias. The motility is given by

$$\mu(\epsilon) = \frac{\mathbf{v} \cdot \hat{\mathbf{n}}}{\epsilon}, \quad (5)$$

where \mathbf{v} and $\hat{\mathbf{n}}$ are vectors whose k^{th} elements denote the (local) velocity at the k^{th} site, and the long time limit of the probability of locating the agent at the k^{th} site, respectively. In practice, we calculate $\hat{\mathbf{n}}$ by constructing the transition matrix associated with the lattice, \mathbf{T} , and then solving $\mathbf{T} \mathbf{n} = \mathbf{n}$ for \mathbf{n} , from which we calculate $\hat{\mathbf{n}} = \mathbf{n}/|\mathbf{n}|$. The elements of \mathbf{T} , $T_{a,b}$, denote the probability that the agent will step from site a to site b per time step. Therefore, \mathbf{T} encodes details about the strength of adhesion/repulsion, the effects of crowding, and the effects of different boundary conditions [21].

The velocity vector, \mathbf{v} , can be calculated element-wise using $v(k) = p_+ L_+ - p_- L_-$, where $v(k)$ is the k^{th} element of \mathbf{v} , p_{\pm} are the probabilities of movement in the positive and negative x directions, $L_{\pm} = 1$ if the relevant target site is vacant and $L_{\pm} = 0$ if the relevant target site is occupied by an obstacle. Once we have applied this method to calculate \bar{D}_x , we perform analogous calculations in the y and z directions to give \bar{D}_y and \bar{D}_z , respectively. Calculating the long time Fickian diffusivity in each direction allows us to investigate the possibility of any anisotropy in the system. For our calculations here, in two dimensions with randomly placed obstacles, we observe no anisotropy and we have $\bar{D}_x \approx \bar{D}_y$ on a sufficiently large lattice. Therefore, we report our results in terms of the total diffusivity, $\bar{D} = \bar{D}_x + \bar{D}_y$ [21]. To demonstrate the accuracy of our calculation, we apply it to the lattice configuration

previously considered in Figure 1(b) and find that $\bar{D} = 0.095$, which is identical to the result obtained using stochastic simulations. To visualise the match between the exact calculation and the simulation results, we superimpose a horizontal line at $\log_{10}(4\bar{D})$ in Figure 1(b), where $\bar{D} = 0.095$ is the exact calculation of the long time Fickian diffusivity. To emphasize the differences between the transport process where obstacles are present ($\phi > 0$) from when obstacles are absent ($\phi = 0$), we plot a horizontal line at $\log_{10}(4D_0)$ in Figure 1(b).

Now that we have explained how the exact calculation of the long time Fickian diffusivity can be performed, we apply the calculation to a family of lattices with different obstacle densities, ϕ . By repeating our calculations of the long time Fickian diffusivity with different values of ζ , we can construct the function $\bar{D}(\phi, \zeta)$, showing how the long time Fickian diffusivity varies with both the obstacle density and the strength of adhesion/repulsion. A contour plot of $\bar{D}(\phi, \zeta)$ is shown in Figure 2(a) for $\zeta \in [-0.9, 0.9]$ and $\phi \in [0, 0.5]$. In this plot we only consider obstacle densities that are below the percolation threshold [22]. When $\phi = 0$ and there are no obstacles, we obtain $\bar{D}(0, \zeta) = D_0$, as expected. Comparing the slope of $\bar{D}(\phi, \zeta)$ in each of the ϕ and ζ directions indicates that, in general, the long time Fickian diffusivity is far more sensitive to ϕ than ζ . In particular, for small values of ϕ , the diffusivity appears, at this scale, to be relatively insensitive to the strength of adhesion/repulsion. However, at larger values of ϕ , there is a significant dependence on ζ .

To further explore the effects of adhesion/repulsion, Figure 2(b) shows the ratio $\bar{D}(\phi, \zeta)/\bar{D}(\phi, 0)$ for different values of ζ . This ratio is approximately unity for all values of ζ when $\phi < 0.3$. For $\phi > 0.3$ the effect of adhesion ($\zeta > 0$) is to decrease $\bar{D}(\phi, \zeta)/\bar{D}(\phi, 0)$, whereas the effect of repulsion ($\zeta < 0$) is to increase $\bar{D}(\phi, \zeta)/\bar{D}(\phi, 0)$, as we might anticipate. The increase in $\bar{D}(\phi, \zeta)$ due to repulsion can be as great as 1100% for the values of ϕ and ζ that we consider.

In summary, we present a method that allows us to quantify the roles of both crowding and adhesion/repulsion by quantifying the long time Fickian diffusivity of a motile agent moving through a crowded environment. A key feature of our approach is that it avoids the need for performing stochastic simulations. Our calculations allow us to examine how the long time Fickian diffusivity depends both on the density of obstacles, ϕ , and the strength of adhesion/repulsion, ζ . Additional results (not presented) confirm the accuracy of our method since the maximum deviation between the exact calculations and estimates based on repeated stochastic simulation results is less than 0.1% for the range of ϕ and ζ considered in Figure 2(a). A key feature of our results is that the long time impact of adhesion/repulsion

is negligible for sufficiently small obstacle densities, $\phi < 0.3$. Therefore, our results suggest that estimates of the long time Fickian diffusivity for low obstacle densities can neglect the affect of adhesion/repulsion. In contrast, for moderate to high obstacle densities, $\phi > 0.3$, our calculations show that adhesion/repulsion has an important impact that ought to be accounted for.

Acknowledgments: This work is supported by the Australian Research Council (DP140100249, FT130100148). We appreciate the assistance and resources provided by the High Performance Computing and Research Support Group at Queensland University of Technology.

-
- [1] MJ Saxton. *Biophys J.* **66** 394 (1994).
 - [2] WS Price, F Tsuchiya, Y Arata. *J. Am. Chem. Soc.* **121** 11503 (1999).
 - [3] DK Wilkins, SB Grimshaw, V Receveur, CM Dobson, JA Jones, LJ Smith. *Biochemistry-US.* **38** 16424 (1999).
 - [4] T Pirzer, M Geisler, T Scheibel, T Hugel. *Phys Biol.* **6** 025004 (2009).
 - [5] DV Nicolau Jr, JF Hancock, K Burrage. *Biophys J.* **92** 1975 (2007).
 - [6] D Lepzelter, MH Zaman. *Biophys J.* **99** L106 (2010).
 - [7] MJ Simpson, C Towne, DLS McElwain, Z Upton. *Phys Rev E.* **82** 041901 (2010).
 - [8] KK Treloar, MJ Simpson, P Haridas, KJ Manton, DI Leavesley, DLS McElwain, RE Baker. *BMC Syst Biol.* **7** 137 (2013).
 - [9] C Deroulers, M Aubert, M Badoual, B Grammaticos. *Phys Rev E.* **79** 031917 (2009) .
 - [10] K Anguige, C Schmeiser. *J Math Biol.* **58** 395 (2009).
 - [11] RN Thompson, CA Yates, RE Baker. *Bull Math Biol.* **74** 2793 (2012).
 - [12] AE Fernando, KA Landman, MJ Simpson. *Phys Rev E.* **81** 011903 (2010).
 - [13] A Wedemeier, H Merlitz, C-X Wu, J Langowski. *J Chem Phys.* **131** 064905 (2009).
 - [14] E Vilaseca, A Isvoran, S Madurga, I Pastor, J Garcés, F Mas. *Phys Chem Chem Phys.* **13** 7396 (2011).
 - [15] T Liggett. *Interacting Particle Systems* (Springer-Verlag) (2005).
 - [16] AJ Ellery, MJ Simpson, SW McCue, RE Baker. *J Chem Phys.* **140** 054108 (2014).

- [17] AJ Ellery, RE Baker, SW McCue, MJ Simpson. *Physica A*. **449** 74 (2016).
- [18] AJ Ellery, RE Baker, MJ Simpson. *J Chem Phys*. **144** 171104 (2016).
- [19] J-F Mercier, GW Slater. *J Chem Phys*. **110** 6050 (1999).
- [20] J-F Mercier, GW Slater. *J Chem Phys*. **110** 6057 (1999).
- [21] AJ Ellery, RE Baker, MJ Simpson. *Phys Biol*. **12** 066010 (2015).
- [22] D Chandler. *Introduction to Modern Statistical Mechanics*. (Oxford: Oxford University Press). (1987).

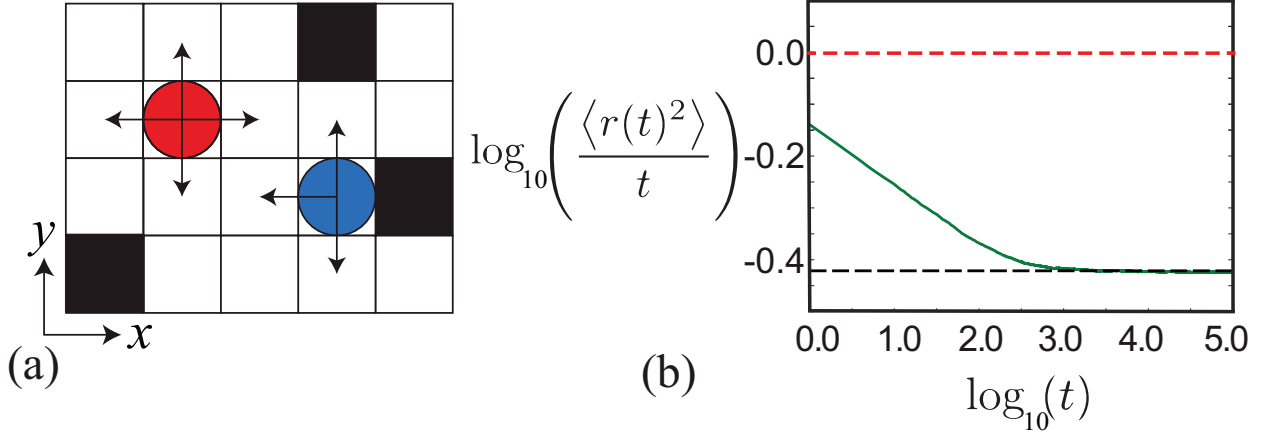


FIG. 1. (a) Lattice schematic illustrating how crowding and adhesion/repulsion are incorporated into the random walk model. Circles represent motile agents and the squares represent immobile obstacles. (b) Plot of $\log_{10}(\langle r^2(t) \rangle / t)$ as a function of $\log_{10}(t)$ (green solid) from a suite of simulations with $p_m = 1.0$, $\zeta = 0$, $\phi = 0.2$, $X = 10$ and $Y = 10$. The ensemble average is obtained by averaging over 100,000 identically prepared realizations. The lower horizontal line (black dashed) shows $\log_{10}(4\bar{D})$, where $\bar{D} = 0.095$ is the exact calculation of the Fickian diffusivity. The upper horizontal line (red dashed) shows $\log_{10}(4D_0)$, for comparison.

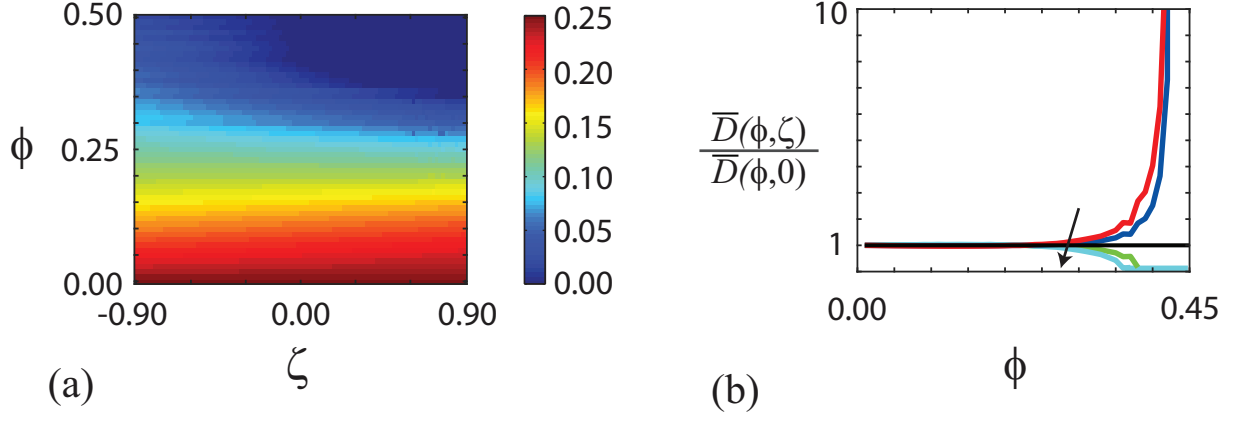


FIG. 2. (a) Plot of $\bar{D}(\phi, \zeta)$ for $\phi \in [0, 0.5]$ and $\zeta \in [-0.9, 0.9]$ with $p_m = 1.0$ and $X = 100$, $Y = 100$. The surface plot of $\bar{D}(\phi, \zeta)$ is constructed by discretizing the (ϕ, ζ) parameter space into a square grid with 50 equally spaced intervals in the ϕ direction and 100 equally spaced intervals in the ζ direction. Values of $\bar{D}(\phi, \zeta)$ are calculated at each discrete (ϕ, ζ) value, and the surface plot is constructed using MATLAB. All exact calculations of $\bar{D}(\phi, \zeta)$ are repeated using 10 identically prepared lattices, randomly populated to density ϕ , and the values of $\bar{D}(\phi, \zeta)$ are averaged over the suite of lattices considered to give the results in (a). Curves in (b) show the ratio $\bar{D}(\phi, \zeta)/\bar{D}(\phi, 0)$ for $\zeta = -0.90$ (red), -0.45 (dark blue), 0.00 (black), 0.45 (green), 0.90 (light blue), with the arrow indicating the direction of increasing ζ .